

# Integration of Shaker-type K<sup>+</sup> channel, KAT1, into the endoplasmic reticulum membrane: Synergistic insertion of voltage-sensing segments, S3–S4, and independent insertion of pore-forming segments, S5–P–S6

Yoko Sato\*, Masao Sakaguchi†, Shinobu Goshima‡, Tatsunosuke Nakamura§, and Nobuyuki Uozumi\*<sup>¶1</sup>

\*Graduate School of Bioagricultural Sciences, and †Bioscience Center, Nagoya University, Nagoya 464-8601, Japan; ‡Department of Molecular Biology, Graduate School of Medical Science, Kyushu University, Fukuoka 812-8582, Japan; and §Faculty of Pharmaceutical Sciences, Chiba University, Chiba 263-8522, Japan

Edited by Lily Y. Jan, University of California, San Francisco, CA, and approved October 10, 2001 (received for review July 31, 2001)

**KAT1 is a member of the Shaker family of voltage-dependent K<sup>+</sup> channels, which has six transmembrane segments (called S1–S6), including an amphipathic S4 with several positively charged residues and a hydrophobic pore-forming region (called P) between S5 and S6. In this study, we systematically evaluated the function of individual and combined transmembrane segments of KAT1 to direct the final topology in the endoplasmic reticulum membrane by *in vitro* translation and translocation experiments. The assay with single-transmembrane constructs showed that S1 possesses the type II signal-anchor function, whereas S2 has the stop-transfer function. The properties fit well with the results derived from combined insertion of S1 and S2. S3 and S4 failed to integrate into the membrane by themselves. The inserted glycosylation sequence at the S3–S4 loop neither prevented the translocation of S3 and S4 nor impaired the function of voltage-dependent K<sup>+</sup> transport regardless of the changed length of the S3–S4 loop. S3 and S4 are likely to be posttranslationally integrated into the membrane only when somewhat specific interaction occurs between them. S5 had the ability of translocation reinitiation, and S6 had a strong preference for N<sub>exo</sub>/C<sub>cyt</sub> orientation. The pore region resided outside because of its lack of its transmembrane-spanning property. According to their own topogenic function, combined constructs of S5–P–S6 conferred the membrane-pore-membrane topology. This finding supports the notion that a set of S5–P–S6 can be independently integrated into the membrane. The results in this study provide the fundamental topogenesis mechanism of transmembrane segments involving voltage sensor and pore region in KAT1.**

**T**he *Arabidopsis thaliana* cDNA, *KAT1*, encodes a hyperpolarization-activated (inward-rectifying) K<sup>+</sup> channel. K<sup>+</sup> is a major nutrient for plants and the most abundant cation in plant cells (1). K<sup>+</sup> channels have been suggested to involve the modulation of K<sup>+</sup> transport in plant cells (2). A number of studies on the structure and function of KAT1 using various heterologous expression systems (3–9) have been reported. Therefore KAT1 is considered as one of the models for inward-rectifying K<sup>+</sup> channels in plants since its gene isolation (4). The membrane topology of KAT1 was determined to contain six transmembrane segments (3), consistent with the model of bacterial K<sup>+</sup> channel and animal Shaker K<sup>+</sup> channel (10, 11). The KAT1 consists of a voltage-sensing motif on the N-terminal side of membrane-pore-membrane structure whose features resemble those of animal Shaker-type voltage-gated K<sup>+</sup> channels (12, 13). Although the final topology of Shaker-type K<sup>+</sup> channels has been determined, there is little topogenesis evidence concerning the formation of the channel structure. The hydrophathy profile of KAT1 shows a relatively low hydrophobicity for S4 and

a highly hydrophobic property for the pore region, which does not explain the final topology of the channel.

Almost all of the integral membrane proteins on the membrane organelles of the exocytic and endocytic pathway are synthesized on the membrane-bound ribosomes and cotranslationally integrated into the membrane, and they acquire their final topology there (14). According to the classification of the topogenic function of transmembrane segments of polytopic membrane proteins, type I and type II signal-anchor sequences (SA-I and SA-II) and stop-transfer (St) sequence have been assigned (15, 16). SA-I transmembrane segments form N<sub>exo</sub>/C<sub>cyt</sub> orientation, and SA-II transmembrane segments form N<sub>cyt</sub>/C<sub>exo</sub> orientation. In general, topogenesis of eukaryotic polytopic membrane protein can be well explained by a simple model (17–19). A series of hydrophobic domains are sequentially integrated by means of the translocon in the endoplasmic reticulum (ER) membrane. The resultant topology preserves the final destination in the cells. On the other hand, a novel membrane integration mode has been identified in the integration process of several proteins: the interaction between transmembrane segments in the insertion step of polytopic membrane proteins causes correct integration of transmembrane segments with weak topogenic functions as reported in band 3 (20), CFTR (21, 22), and CLC chloride channel (23).

To understand and evaluate the mechanism of the integration process of KAT1, we evaluated the preference of the orientation and ability of each transmembrane segment and the coordinated insertion of transmembrane segments consisting of KAT1.

## Materials and Methods

***In Vitro* Transcription, Translation, and Translocation.** Each PCR-amplified fragment was subcloned into the corresponding sites in the plasmids that were used for topogenic assay (24). The fragments contained both the flanking cytoplasmic and extracellular loops [S1 (R48–D95), S2 (Y85–R132), S3 (D116–S168), S4 (S152–T205), S5 (E186–Y235), Pore (W230–D277), and S6 (Y263–A315)] (Fig. 9, which is published as supporting information on the PNAS web site, www.pnas.org). The DNA sequence containing N-glycosylation sites derived from human bands 3 (24) was substituted for the corresponding sequence in

This paper was submitted directly (Track II) to the PNAS office.

Abbreviations: ER, endoplasmic reticulum; PL, prolactin; RM, rough microsomal membrane; SA-I, type I signal-anchor sequence; SA-II, type II signal-anchor sequence, St, stop-transfer.

<sup>¶</sup>To whom reprint requests should be addressed. E-mail: uozumi@agr.nagoya-u.ac.jp.

The publication costs of this article were defrayed in part by page charge payment. This article must therefore be hereby marked "advertisement" in accordance with 18 U.S.C. §1734 solely to indicate this fact.

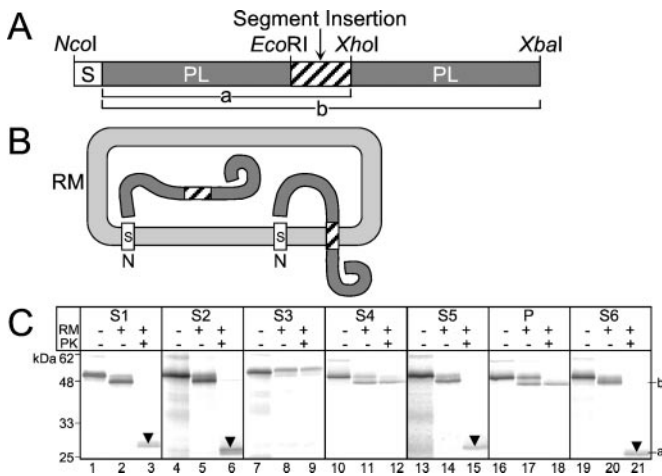


**Fig. 1.** St function of each possible transmembrane segment in KAT1. (A) The model protein for the systematic assessment of St function. The signal peptide (S) of PL, PL, the inserted segments, and the second PL were sequentially arranged. a and b show the molecular mass in C. (B) Possible transmembrane topologies in the constructs. (C) The representative results of *in vitro* experiments. The model proteins were expressed *in vitro* in the absence (-) or presence (+) of RM. The aliquots were treated with proteinase K (PK+). The proteins were subjected to SDS/12.5% PAGE followed by an image analysis. The stop-transferred form and the fully translocated form are indicated by a with arrowheads and b, respectively.

the plasmid constructed previously for KAT1 expression by the two-step PCR approach (5) and the method developed by Kunkel (25). To yield prolactin (PL) fusions, the DNA encoding S1-2 (M1-R132), S1-3 (M1-S168), S1-4 (M1-T205), and S1-5 (M1-Y235) was fused to the PL fragment with or without the N-glycosylation acceptor sequence (PL or PL<sub>gly</sub>) in the plasmid constructed by Ota *et al.* (24). The RNAs were translated in reticulocyte lysate (24, 26, 27) in either the absence or presence of rough microsomal membranes (RMs) from dog pancreas (24, 28). After translation, the aliquots were treated with proteinase K (200 μg/ml).

**Recording of Ion Currents in *Xenopus laevis* Oocytes.** Capped complementary RNA was injected into *X. laevis* oocytes prepared as described (7). The oocytes were kept for 1-2 days at 18°C in a solution as described (5). The two-electrode voltage clamping recordings were performed in a solution containing 6 mM MgCl<sub>2</sub>, 1.8 mM CaCl<sub>2</sub>, 100 mM KCl, 10 mM Hepes-HCl, pH 7.3. Voltage-pulse protocols, data acquisition, and data analysis were performed by using a voltage clamp amplifier (AxoClamp 2B, Axon Instruments, Foster City, CA) and software (PCLMP6, Axon Instruments).

## Results

**Assessment of the St Function.** First, we examined whether or not each transmembrane segment (S1 to S6) can interrupt the ongoing translocation through the translocon and eventually become a transmembrane segment, that is, possess the St function. The assessment of a St function was carried out essentially as described by Kuroiwa *et al.* (29) using the systematically constructed model proteins (Fig. 1A and B). Translocation was initiated by the amino-terminal signal peptide, which leads to the translocation of its C-terminus end. If the inserted transmembrane segment shows the St function, the carboxyl-terminal half is exposed on the cytoplasmic side of the membrane, where the fused PL domain is hydrolyzed by externally added proteinase K (Fig. 1B Right). If the inserted transmembrane segment does not show the St function, the nascent polypeptide should remain in the luminal space, where it becomes fully resistant to the externally added proteinase K (Fig. 1B

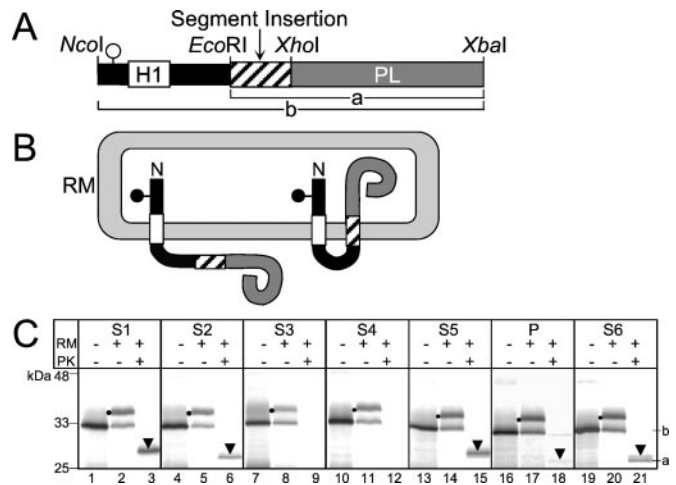


**Fig. 2.** Translocation initiation function of each possible transmembrane segment in KAT1. The symbols are the same as in Fig. 1. (A) The model protein for the systematic assessment of translocation initiation function. The SA-I of *E. coli* leader peptidase (H1) preceding the domain with the N-glycosylation site (○), the inserted segments, and the PL were sequentially arranged. (B) Possible transmembrane topologies in the constructs. (C) The representative results of *in vitro* experiments. The glycosylated forms are indicated by dots.

*Left*). The model proteins were synthesized in the absence of RM as single bands with the expected molecular mass (Fig. 1C, lanes 1, 4, 7, 10, 13, 16, and 19). When synthesized in the presence of RM, they were processed into mature forms (b in Fig. 1C). The proteinase K treatment gave rise to truncated fragments (arrowheads at position a in Fig. 1C). The membrane-protected truncated forms were degraded by proteinase K in the presence of a detergent (data not shown). Because the insertion of S3 contains a potential glycosylation site (NGS at positions 158-160, Fig. 9), the S3 construct was efficiently glycosylated in the presence of RM and the full length of the product became resistant to proteinase K treatment, indicating that the S3 segment did not stop the translocation (Fig. 1C, lanes 8 and 9). S1, S2, S5, and S6 showed a high St function with 95%, 93%, 92%, and 100%, respectively (Figs. 1C and 10A,

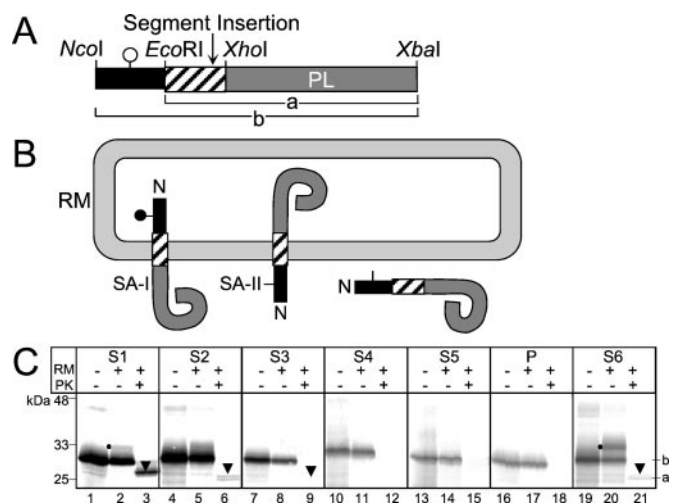


**Fig. 3.** Nexo/Cyt (SA-I) or Ncyt/Cexo (SA-II) topogenic function of each possible transmembrane segment in KAT1. The symbols are the same as in Fig. 1. (A) The model protein for the systematic assessment of translocation initiation function. The N-glycosylation loop (○) of band 3, each segment, and the PL were sequentially arranged. (B) Possible transmembrane topologies in the constructs. (C) The representative results of *in vitro* experiments.

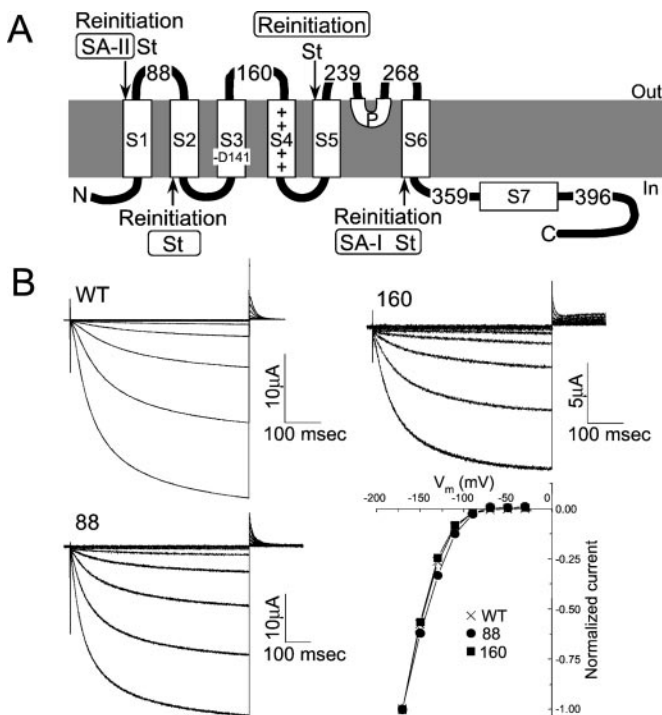


**Fig. 4.** The characterization of topogenic function of each segment and the insertion of N-glycosylation sites in the loops. (A) The summary of the topogenic function of each segment determined from Figs. 1–3. Each N-glycosylation loop is inserted at the C-terminal end of the numbered residues. (B) Time courses of currents in oocytes injected with mRNA of wild type (WT) and KAT1 containing the N-glycosylation sites at positions 88 or 160. Holding potential was  $-30$  mV, and step command pulses from  $-30$  mV to  $-170$  mV with  $-20$ -mV increments. The KAT1 containing the N-glycosylation sequence at positions 239 or 268 did not confer the  $K^+$  channel function in *X. laevis* oocytes. Currents were obtained at the end of each step pulse and normalized (currents at  $-150$  mV were taken as  $-1$ ) to compare  $I$ - $V$  relation among curves for WT and KAT1 with N-glycosylation at positions 88 and 160.

which is published as supporting information on the PNAS web site). If all transmembrane segments in KAT1 integrate according to the simple model (18, 19), St function is essential in even-numbered segments. Because S4 does not possess St function, S4 is likely to integrate by a process different from the simple model.

**Assessment of the Translocation Initiation Function.** We assessed the reinitiation function of the membrane segments with the series of the model proteins. For these experiments (Fig. 2A and B), the H1 was integrated into the membrane as SA-I, whose function can be confirmed by the appearance of N-glycosylated bands (24). The glycosylated bands appeared in experiments with all of the constructs (dots in Fig. 2C). If the inserted transmembrane segment reinitiates the translocation of the following domain, the carboxyl-terminal PL domain should become proteinase K resistant (Fig. 2B). After the proteinase K treatment, the constructs of S1, S2, S5, and S6 gave substantial amounts of the truncated form (arrowheads at position a; Figs. 2C and 10B), which implies that they contain the reinitiation functions. The lack of the reinitiation function in S3 suggests that this segment is integrated into the membrane by a mechanism that differs from the simple model.

**Assessment of Membrane Segments for Signal-Anchor Sequence.** The orientation ( $N_{\text{exo}}/C_{\text{cyt}}$  or  $N_{\text{cyt}}/C_{\text{exo}}$ ) of all of the segments was examined by using model proteins (Fig. 3A and B). If the segment shows the SA-I function, the amino-terminal portion is

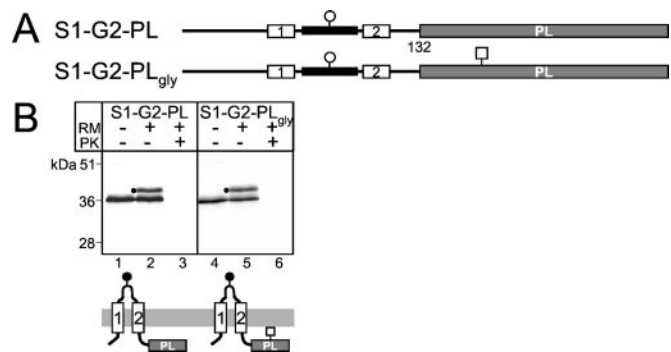


**Fig. 5.** Initiation function of S1 leads to membrane insertion of the following segment, S2. (A) PL or PL<sub>gly</sub> was fused to the end of N-terminal regions containing S1 and S2. N-glycosylation sequence (G) was placed in the S1–S2 loop. The possible glycosylation sites in the loop of KAT1 and PL are shown by  $\circ$  and  $\square$ , respectively. The number of residues in KAT1 fused with PL is indicated. (B) Membrane topogenesis of S1 and S2 in *in vitro* system. The glycosylated bands are shown as dots. (Lower) Shown are the topologies deduced from the results. Glycosylated and nonglycosylated sites are shown as closed and open symbols, respectively.

translocated and glycosylated. If it shows the SA-II function, the PL is translocated and becomes proteinase K resistant but the N-terminal domain is not glycosylated. When synthesized in the presence of RM, only the construct with S6 gave an apparent glycosylated band (dots in Figs. 3C and 10C). Although glycosylated bands from the construct with S1 could be detected to a lesser extent, a large amount of the proteinase K-resistant bands was observed (Figs. 3C and 10C), indicating that S1 showed an efficient SA-II function. S2 and S3 possess very weak SA-II function (Fig. 10C). S6 exhibited a strong SA-I tendency compared with an SA-II function (Fig. 10C). The construct with S5 and P gave neither a glycosylated band nor a proteinase K-resistant fragment, indicating the absence of signal functions in this construct.

The characteristics of each of the S1–S6 fragments are summarized in Fig. 4A. When the insertion order in their translocation step in the ER membrane is considered, it seems reasonable that S1 and S2 have SA-II function and St function, respectively. The reinitiation function for S5 and St and/or SA-I function for S6 are inevitable to assume the final KAT1 membrane topology. P did not show strong properties for these functions, supporting the evidence that P does not act as a transmembrane segment in the final topology. On the other hand, the most striking finding from the above results is that neither S3 nor S4 possess topogenic functions. This finding indicates that the integration of S3 and S4 cannot be explained by classical sequential insertion mode.

**Insertion of N-Glycosylation Sites for Transmembrane Mapping.** To map the extracellular loops of KAT1, the N-glycosylation acceptor sequence from human band 3 (30) was inserted into each loop of KAT1 (5) as shown in Fig. 4A. N-glycosylation occurs on the luminal side of the ER, which is the extracellular side of the protein when it is disposed to the plasma membrane. In the wild-type KAT1, a consensus N-glycosylation site (NGS at residues 158–160) exists in the loop of S3–S4. However, the site was not subjected to N-glycosylation (Fig. 11, which is published as supporting information on the PNAS web site). In the construct with insertion at 160, N158 was replaced with Gln (Q) in the KAT1 to avoid unexpected occurrence of the glycosylation at N158. N-glycosylation occurred in the constructs with the insertion at 88, 160, 239, and 268 (Fig. 11).

To evaluate the influence of the insertion of the glycosylation acceptor site on the structure of KAT1, we measured the ion transport capability of the protein in *X. laevis* oocytes by voltage

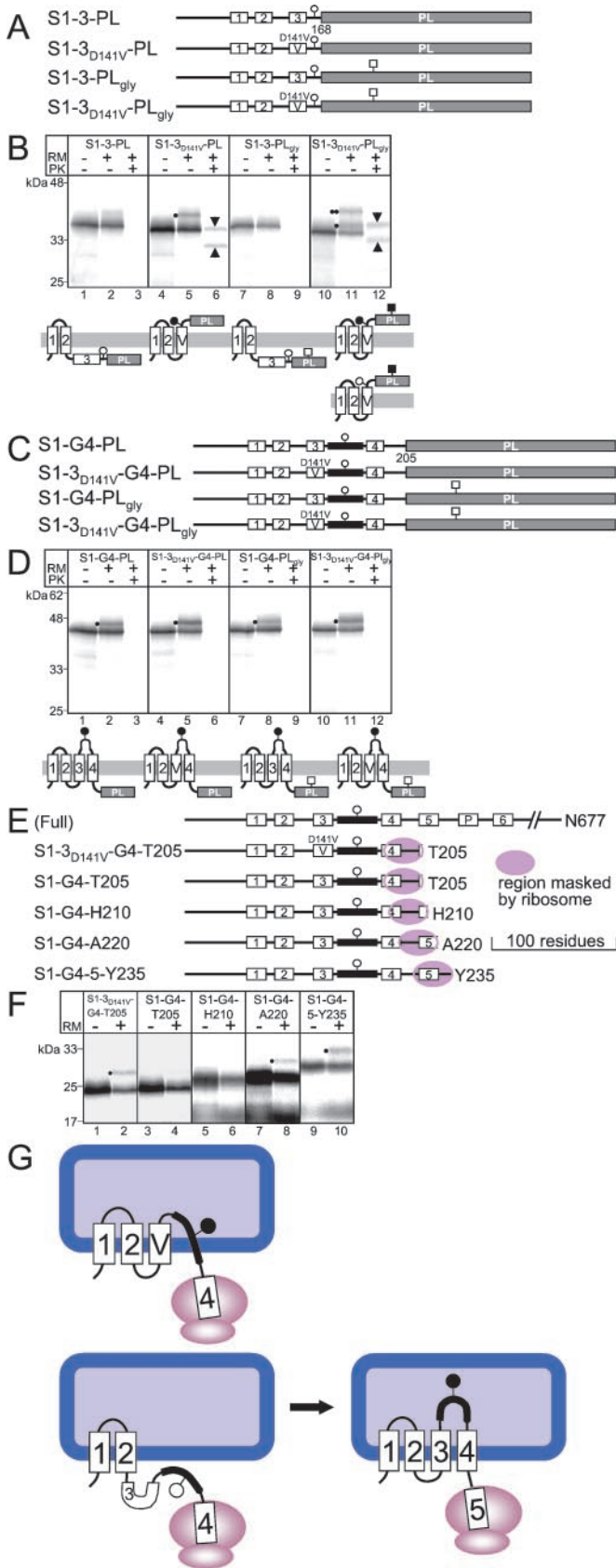


**Fig. 6.** Synergistic integration of S3 and S4 occurs posttranslationally. The symbols are the same as those in Fig. 5. (A) PL or PL<sub>gly</sub> was fused to the end of N-terminal regions containing S1–S3. The S3 with D141V is indicated by V. The endogenous N-glycosylated residues at position 158 exist in the constructs. (B)

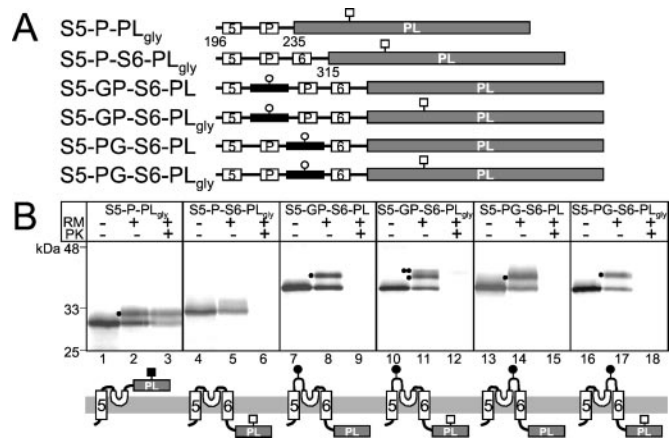


**Fig. 7.** S5–P–S6 can be arranged into a proper topology without S1–S4. The symbols are the same as those in Fig. 6. (A) The regions from S5 through S6 were fused to PL or PL<sub>gly</sub>. N-glycosylation sequence was placed in the S5–P loop or the P–S6 loop. (B) Membrane topogenesis of S5, P, and S6 by *in vitro* system. The monoglycosylated and diglycosylated forms are indicated by single and double dots, respectively.

clamp recordings. Inward currents remained unaffected by the insertion of N-glycosylation acceptor sequences at 88 and 160 (Figs. 4B and 11). In contrast, the insertion at 239 in the S5–P loop and at 268 in the P–S6 loop abolished the function of KAT1 in *X. laevis* oocytes. The sites are so close to pore-forming regions that the insertion is likely to disorder the function of K<sup>+</sup> transport. Hydropathy profile of KAT1 shows an additional highly hydrophobic region (called S7 in Figs. 4A and 11) between residues 359 and 396. We confirmed that the S7 does not become a transmembrane segment by the N-glycosylation approach with the constructs containing the N-glycosylation site between 359 and 360 or between 396 and 397 (Fig. 11).

**The Membrane Integration of S1 and S2 Matches with the Simple Model for Membrane Topogenesis.** Because S2 has a St function but not an SA-I function (Figs. 1, 3, and 4), we assumed that the presence of S1 is requisite to insertion of S2 into the membrane. We examined the combinational integration of S1 and S2 by using the constructs of the glycosylated acceptor site in the S1–S2 loop (Fig. 5A). When translated in the presence of RM, both S1–G2–PL and S1–G2–PL<sub>gly</sub> fusion gave an additional glycosylated form and all bands were completely degraded by proteinase K (Fig. 5B). These results demonstrate that S2 acts as an efficient St segment and takes a proper membrane topology for KAT1 when the preceding signal-anchor sequence of S1 exists in the construct.

**S4 Assists Membrane Integration of S3.** Because individual S3 and S4 have no topogenic functions (Figs. 1–3 and 4A), the interaction between transmembrane segments seems to be necessary for their insertion into the membrane. We examined how S3 and S4 are inserted into the membrane by using several fusion constructs (Fig.

Assay of the constructs by *in vitro* system. The proteinase K-resistant bands are shown by arrowheads. (C) PL or PL<sub>gly</sub> was fused to the end of N-terminal regions containing S1–S4. The endogenous N-glycosylated residue at position 158 was removed. (D) Assay of the constructs by *in vitro* system. (E) Requirement of S4 for membrane integration of S3. The synthesized mRNAs do not possess a stop codon so that the nascent polypeptides remain as peptidyl-tRNA and are not released from the ribosomes. The endogenous N-glycosylated residue at position 158 was removed. (F) Detection of N-glycosylated bands in the ER membrane based on the results of F. After S4 is released from the ribosome complex, S3 and S4 are inserted into the ER membrane.

6). When translated in the presence of RM, both S1–3–PL and S1–3–PL<sub>gly</sub> fusion gave none or very weak glycosylated bands (Fig. 6B, lanes 2 and 8). By the protease protection assay, all bands disappeared completely. These results confirmed that S3 did not show integration function even when placed after the S1 and S2 as in the natural context. In the middle of S3, a negatively charged residue at position 141 (D141) exists. This residue is conserved in other Shaker-type ion channels (31). The neutralization of the corresponding charge is reported to be necessary for correct integration of S3 (3, 32). The conversion of D141 to valine (D141V) resulted in the appearance of a single glycosylated band in S1–3<sub>D141V</sub>–PL (Fig. 6B, lane 5) and double-glycosylated band in S1–3<sub>D141V</sub>–PL<sub>gly</sub> (Fig. 6B, lane 11). The subsequent proteinase K treatment yielded two bands (Fig. 6B, lanes 6 and 12). These results indicated that the D141V mutation gave the reinitiation function to S3 and resulted in the glycosylation of N158 and PL domain. If the glycosylation efficiency of PL<sub>gly</sub> is estimated to be almost 100%, the glycosylation efficiency of the endogenous glycosylation site in these constructs, N158, is considered to be about 50% from the result of Fig. 6B, lane 6. The low level of the glycosylation is highly likely to be caused by proximity to the membrane. According to the explanation, the glycosylation at PL<sub>gly</sub> quantitatively shifted the two bands in Fig. 6B, lane 6 up to upper positions in Fig. 6B, lane 12. Because S1 and S2 can be integrated by themselves (Fig. 5), the results suggested that the integration of S3 requires the subsequent amino acid sequences.

We exploited the role of S4 on integration of S3 into the membrane by using fusion constructs (Fig. 6C). When translated in the presence of RM, all constructs, S1–G4–PL, S1–3<sub>D141V</sub>–G4–PL, S1–G4–PL<sub>gly</sub>, and S1–3<sub>D141V</sub>–G4–PL<sub>gly</sub> showed a single glycosylated band. From both PL<sub>gly</sub>-containing constructs, double-glycosylated bands could not be detected. The proteinase K treatment resulted in an almost complete degradation of all constructs. The replacement of D141V enhanced the intensity of N-glycosylated bands (Fig. 6D). These results indicate that the insertion of S3 into the membrane requires S4. Interestingly, in these constructs, S4 was not translocated into ER lumen through the membrane but was retained in the membrane despite its highly charged character.

To test that the insertion of S3 is constrained by the exposure of S4 from ribosome-mRNA complex, we constructed a series of truncated fusion proteins as shown in Fig. 6E. Because the constructs lacked the stop codon in the mRNA, the synthesized polypeptides could not be released from ribosomes. In general, the distance between ribosomes and the translocon is estimated to be about 30–40 aa (33) (Fig. 6E). In the control, glycosylated bands from S1–3<sub>D141V</sub>–G4–T205 were observed (Fig. 6F). This finding clearly implies that the glycosylation site of the nascent polypeptide chain of 205 residues can reach the active site of oligosaccharyl transferase. In this context, the distance from the glycosylation site in the band 3 loop to the C-terminus peptidyl site in the ribosome is estimated to be 68 residues in length. S1–G4–T205 has enough space for the N-glycosylation if S3 acts as a transmembrane segment (Fig. 6F and G). Nevertheless, S1–G4–T205, and S1–G4–H210 were not glycosylated (Fig. 6F). S1–G4–A220 and S1–G4–5–Y235 became glycosylated (Fig. 6F). We conclude therefore that S3 and S4 are synergistically integrated by a posttranslational manner, only when S4 emerges from the ribosome (Fig. 6G). This finding strongly suggests that specific interaction between S3 and S4 is a critical event for their membrane integration.

**S5, P, and S6 Can Integrate Properly Without S1–S4.** S5–P–S6 structure in KAT1 shares the same membrane–pore–membrane structure with a simple K<sup>+</sup> channel with two transmembrane segments (M1 and M2) and a pore region (4, 12, 13, 34, 35). Hence, we postulated that S5–P–S6 could take a proper membrane topology without the preceding S1–S4 in KAT1. To evaluate this concept and

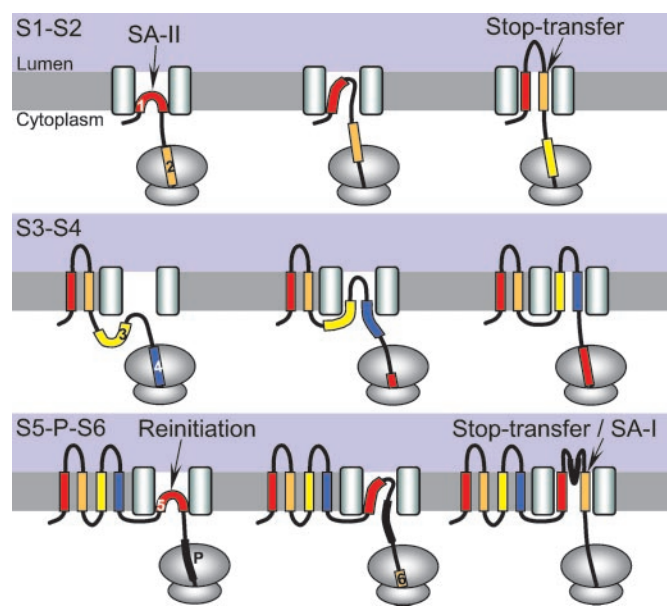


**Fig. 8.** Topogenesis of KAT1. S1–S2 is inserted sequentially into the membrane (Top). S3–S4 is synergistically inserted by a posttranslational manner (Middle). Reinitiation function of S5 leads to proper membrane formation of S5–P–S6 independently of the preceding transmembrane segments (Bottom).

to study the membrane topogenesis of S5–P–S6, the fusion proteins were constructed as shown in Fig. 7A. The first methionine was introduced at the C-terminal residue of the predicted S4 (from I196) in the constructs to possess only the cytosolic amino acids in the S4–S5 loop in the resultant proteins. From S5–P–PL<sub>gly</sub> construct, an N-glycosylated band was observed in the presence of RM and the band was well protected from proteinase K treatment. In the case of S5–P–S6–PL<sub>gly</sub>, most bands were digested by proteinase K treatment (Fig. 7B). To confirm the results, N-glycosylation acceptor sites were generated between S5 and P or between P and S6 (Fig. 7A). The sites were strongly glycosylated, and a glycosylation site located inside PL<sub>gly</sub> had none or small intensive glycosylated bands (Fig. 7B). Moreover, all these bands disappeared after proteinase K treatment. Although the insertions of N-glycosylation acceptor sequence in S5–P or in P–S6 impair the KAT1 function (Figs. 4B and 11A), the insertion did not affect the membrane topology of S5–P–S6. S5 can be integrated into the membrane by itself regardless of the absence of S1–S4, and S6 takes a proper membrane orientation. These results are consistent with the topogenesis properties of S5, P, and S6 as determined in Figs. 1–3.

## Discussion

The data reported here demonstrate that transmembrane regions of KAT1 possess unequal topogenic functions. S1, S2, S5, and S6 in KAT1 have the reinitiation functions in odd-numbered transmembrane segments and the St functions of even-numbered transmembrane segments (Figs. 1–3 and 4A), which is consistent with a widely accepted model for the membrane integration of general multispinning membrane proteins (17–19). On the other hand, insufficient topogenic functions for S3 and S4 necessitates that an alternative topogenic model explain their membrane integration.

S1 and S2 showed the typical topogenic properties, which fit well with the simple model. S1 inserts into membrane and retains in the membrane as a signal anchor, and the following S2 is integrated as a St sequence (Figs. 5 and 8). S1 also has SA-I function, but the several positively charged residues located proximal to S1 may stabilize the N terminus of S1 at the cytosolic side with respect to the membrane, which allows S1 to take the

$N_{\text{cyt}}/C_{\text{exo}}$  orientation (SA-II function) in KAT1. The formation of S1 and S2 in the membrane provides a firm base for the following S3 and S4 insertion.

KAT1 shares typical similarity with other animal and plant  $K^+$  channels, in the aspartic acid residue located in the middle of S3 and several positively charged residues of S4 which serve as a voltage sensor (31). Tu *et al.* (36) have reported that S3 has a translocation activity through the membrane and S4 has an integration activity in Kv1.3, which is different from our results. The assay with single-transmembrane constructs (Figs. 1–3 and 4A) reveals that S3 alone lacks the ability to integrate into the membrane. The poor translocation efficiency for S3 is consistent with the results observed in the *E. coli* system (3). The conversion of the negatively charged aspartic acid to the valine (D141V) led S3 into *E. coli* membrane. Likewise, increase in the translocation efficiency of S3 with D141V was observed in this study (Fig. 6). Taken together, the charge of D141 is likely to prevent S3 insertion into the membrane by itself. Masking the charge of D141 by pairing with a positive residue in S4 enable the S3–S4 posttranslational insertion into the membrane when the positively charged S4 is released from the ribosome-mRNA complex (Fig. 6 E–G).

Another intriguing finding in this study is that S4 has no St functions (Fig. 1) but once S4 entered the membrane in the presence of S1–S3, S4 was not released into the lumen. In addition, even after the removal of the charge from residue at position 141 in S3 (S1–S<sub>D141V</sub>–G4), S4 was still allowed to span the membrane (Fig. 6 C and D). This finding suggests that intramolecular interactions between positive residues in S4 and aspartic acid at positions 95 or 105 in S2 may contribute to the retention of S4 in the

membrane; S2, S3, and S4 are considered to be components of the voltage sensor as demonstrated in animal  $K^+$  channels (37–39).

The space requirements for access of oligosaccharyl transferase in the ER membrane have been reported (40, 41). The endogenous consensus N-glycosylation site at position 158 did not meet the requirement (Fig. 11). The insertion of the N-glycosylation acceptor sequence in the S3–S4 loop did not impair the function of voltage-dependent  $K^+$  transport (Figs. 4B and 11A). The recent evidence in animal Shaker-type  $K^+$  channels shows that the movement of the charges of S3 and S4 is smaller than the predicted sliding helix model (42–44). In fact, the increasing or decreasing length of loop of S3–S4 in Shaker  $K^+$  channels preserved the voltage movement for functional  $K^+$  transport (11, 45, 46). The length of the S3–S4 loop might not be critical for the voltage sensor operation in Shaker-type  $K^+$  channels.

This study also demonstrates that S1–S4 can be integrated independently of S5–P–S6 (Fig. 6 C and D) and S5–P–S6 can be arranged into a proper topology without the preceding segments S1–S4 (Fig. 7). This result supports the notion that the S5–P–S6 structure in KAT1 corresponds to an membrane-pore-membrane structure in an ancestral  $K^+$  channel structure (12). In Kv1.3, peptides containing S6 and the following C-terminus region were completely translocated across the membrane (36). In contrast, the reinitiation function of S5 and not only St function but also SA-I function of S6 in KAT1 may contribute to achieve the final topology for membrane-pore-membrane structure.

This work was supported by grants-in-aid for Center of Excellence (COE) research to N.U. and for scientific research to N.U. (Grants 13206032 and 13660088) and to M.S (Grants 11480168 and 13208024) from the Ministry of Education, Science, Sports, and Culture of Japan.

1. Fox, T. C. & Guerinot, M. L. (1998) *Annu. Rev. Plant Physiol. Plant Mol. Biol.* **49**, 669–696.
2. Rodríguez-Navarro, A. (2000) *Biochim. Biophys. Acta* **1469**, 1–30.
3. Uozumi, N., Nakamura, T., Schroeder, J. I. & Muto, S. (1998) *Proc. Natl. Acad. Sci. USA* **95**, 9773–9778.
4. Anderson, J. A., Huprikar, S. S., Kochian, L. V., Lucas, W. J. & Gaber, R. F. (1992) *Proc. Natl. Acad. Sci. USA* **89**, 3736–3740.
5. Uozumi, N., Gassmann, W., Cao, Y. & Schroeder, J. I. (1995) *J. Biol. Chem.* **270**, 24276–24281.
6. Nakamura, R. L., Anderson, J. A. & Gaber, R. F. (1997) *J. Biol. Chem.* **272**, 10111–10118.
7. Schachtman, D. P., Schroeder, J. I., Lucas, W. J., Anderson, J. A. & Gaber, R. F. (1992) *Science* **258**, 1654–1658.
8. Marten, I., Gaymard, F., Lemaillet, G., Thibaud, J. B., Sentenac, H. & Hedrich, R. (1996) *FEBS Lett.* **380**, 229–232.
9. Uozumi, N. (2001) *Am. J. Physiol.* **281**, C733–C739.
10. Johansson, M. & von Heijne, G. (1996) *J. Biol. Chem.* **271**, 25912–25915.
11. Shih, T. M. & Goldin, A. L. (1997) *J. Cell Biol.* **136**, 1037–1045.
12. Durell, S. R., Hao, Y., Nakamura, T., Bakker, E. P. & Guy, H. R. (1999) *Biophys. J.* **77**, 775–788.
13. Kato, Y., Sakaguchi, M., Mori, Y., Saito, K., Nakamura, T., Bakker, E. P., Sato, Y., Goshima, S. & Uozumi, N. (2001) *Proc. Natl. Acad. Sci. USA* **98**, 6488–6493. (First Published May 8, 2001; 10.1073/pnas.101556598)
14. Sakaguchi, M. (1997) *Curr. Opin. Biotechnol.* **8**, 595–601.
15. Sakaguchi, M., Tomiyoshi, R., Kuroiwa, T., Mihara, K. & Omura, T. (1992) *Proc. Natl. Acad. Sci. USA* **89**, 16–19.
16. High, S. & Dobberstein, B. (1992) *Curr. Opin. Cell Biol.* **4**, 581–586.
17. Blobel, G. (1980) *Proc. Natl. Acad. Sci. USA* **77**, 1496–1500.
18. Matlack, K. E., Mothes, W. & Rapoport, T. A. (1998) *Cell* **92**, 381–390.
19. Hegde, R. S. & Lingappa, V. R. (1997) *Cell* **91**, 575–582.
20. Ota, K., Sakaguchi, M., Hamasaki, N. & Mihara, K. (2000) *J. Biol. Chem.* **275**, 29743–29748.
21. Tector, M. & Hartl, F. U. (1999) *EMBO J.* **18**, 6290–6298.
22. Lu, Y., Xiong, X., Helm, A., Kimani, K., Bragin, A. & Skach, W. R. (1998) *J. Biol. Chem.* **273**, 568–576.
23. Schmidt-Rose, T. & Jentsch, T. J. (1997) *Proc. Natl. Acad. Sci. USA* **94**, 7633–7638.
24. Ota, K., Sakaguchi, M., Hamasaki, N. & Mihara, K. (1998) *J. Biol. Chem.* **273**, 28286–28291.
25. Kunkel, T. A. (1985) *Proc. Natl. Acad. Sci. USA* **82**, 488–492.
26. Sakaguchi, M., Hachiya, N., Mihara, K. & Omura, T. (1992) *J. Biochem. (Tokyo)* **112**, 243–248.
27. Jackson, R. J. & Hunt, T. (1983) *Methods Enzymol.* **96**, 50–74.
28. Walter, P. & Blobel, G. (1983) *Methods Enzymol.* **96**, 84–93.
29. Kuroiwa, T., Sakaguchi, M., Mihara, K. & Omura, T. (1991) *J. Biol. Chem.* **266**, 9251–9255.
30. Ota, K., Sakaguchi, M., von Heijne, G., Hamasaki, N. & Mihara, K. (1998) *Mol. Cell* **2**, 495–503.
31. Jan, L. Y. & Jan, Y. N. (1992) *Cell* **69**, 715–718.
32. Henn, D. K., Baumann, A. & Kaupp, U. B. (1995) *Proc. Natl. Acad. Sci. USA* **92**, 7425–7429.
33. Matlack, K. E. & Walter, P. (1995) *J. Biol. Chem.* **270**, 6170–6180.
34. Kubo, Y., Baldwin, T. J., Jan, Y. N. & Jan, L. Y. (1993) *Nature (London)* **362**, 127–133.
35. Doyle, D. A., Morais Cabral, J., Pfuetzner, R. A., Kuo, A., Gulbis, J. M., Cohen, S. L., Chait, B. T. & MacKinnon, R. (1998) *Science* **280**, 69–77.
36. Tu, L., Wang, J., Helm, A., Skach, W. R. & Deutsch, C. (2000) *Biochemistry* **39**, 824–836.
37. Papazian, D. M., Shao, X. M., Seoh, S. A., Mock, A. F., Huang, Y. & Wainstock, D. H. (1995) *Neuron* **14**, 1293–1301.
38. Larsson, H. P., Baker, O. S., Dhillon, D. S. & Isacoff, E. Y. (1996) *Neuron* **16**, 387–397.
39. Seoh, S. A., Sigg, D., Papazian, D. M. & Bezanilla, F. (1996) *Neuron* **16**, 1159–1167.
40. Popov, M., Tam, L. Y., Li, J. & Reithmeier, R. A. (1997) *J. Biol. Chem.* **272**, 18325–18332.
41. Nilsson, I., Sääf, A., Whitley, P., Gafvelin, G., Waller, C. & von Heijne, G. (1998) *J. Mol. Biol.* **284**, 1165–1175.
42. Durell, S. R. & Guy, H. R. (1992) *Biophys. J.* **62**, 238–247; discussion 247–250.
43. Cha, A., Snyder, G. E., Selvin, P. R. & Bezanilla, F. (1999) *Nature (London)* **402**, 809–813.
44. Glauner, K. S., Mannuzzu, L. M., Gandhi, C. S. & Isacoff, E. Y. (1999) *Nature (London)* **402**, 813–817.
45. Gonzalez, C., Rosenman, E., Bezanilla, F., Alvarez, O. & Latorre, R. (2000) *J. Gen. Physiol.* **115**, 193–208.
46. Sørensen, J. B., Cha, A., Latorre, R., Rosenman, E. & Bezanilla, F. (2000) *J. Gen. Physiol.* **115**, 209–222.